Published in final edited form as:
Mol Cell. 2013 January 10; 49(1): 18–29. doi:10.1016/j.molcel.2012.10.015.

ALKBH5 Is a Mammalian RNA Demethylase that Impacts RNA Metabolism and Mouse Fertility

Guanqun Zheng[1,11], **John Arne Dahl**[3,11], **Yamei Niu**[2,11], **Peter Fedorcsak**[4], **Chun-Min Huang**[2], **Charles J. Li**[1], **Cathrine B. Vågbø**[6], **Yue Shi**[2,7], **Wen-Ling Wang**[2,7], **Shu-Hui Song**[5], **Zhike Lu**[1], **Ralph P.G. Bosmans**[1], **Qing Dai**[1], **Ya-Juan Hao**[2,7], **Xin Yang**[2,7], **Wen-Ming Zhao**[5], **Wei-Min Tong**[8], **Xiu-Jie Wang**[9], **Florian Bogdan**[3], **Kari Furu**[3], **Ye Fu**[1], **Guifang Jia**[1], **Xu Zhao**[2,7], **Jun Liu**[10], **Hans E. Krokan**[6], **Arne Klungland**[3,*], **Yun-Gui Yang**[2,7,*], and **Chuan He**[1,*]

[1]Department of Chemistry, Institute for Biophysical Dynamics, The University of Chicago, 929 East 57th Street, Chicago, IL 60637, USA

[2]Genome Structure & Stability Group, BIG CAS-OSLO Genome Research Cooperation, Disease Genomics and Individualized Medicine Laboratory, Beijing Institute of Genomics, Chinese Academy of Sciences, No.7 Beitucheng West Road, Chaoyang District, Beijing 100029, P.R. China

[3]Centre for Molecular Biology and Neuroscience, Institute of Medical Microbiology, BIG CAS-OSLO Genome Research Cooperation, Oslo University Hospital, Oslo 0027, Norway

[4]Department of Gynecology, Oslo University Hospital, Rikshospitalet, Oslo 0027, Norway

[5]Core Genomic Facility, Beijing Institute of Genomics, Chinese Academy of Sciences, No.7 Beitucheng West Road, Chaoyang District, Beijing 100029, P.R. China

[6]Department of Cancer Research and Molecular Medicine, Norwegian University of Science and Technology, 7489 Trondheim, Norway

[7]University of Chinese Academy of Sciences, 19A Yuquan Road, Beijing 100049, P.R. China

[8]Department of Pathology and Center for Experimental Animal Research, Institute of Basic Medical Sciences, Chinese Academy of Medical Sciences and Peking Union Medical College, 5 Dong Dan San Tiao, Beijing 100005, P.R. China

[9]Institute of Genetics and Developmental Biology, Chinese Academy of Sciences, No.1 West Beichen Road, Chaoyang District, Beijing 100101, P.R. China

[10]College of Chemistry and Molecular Engineering and Synthetic and Functional Biomolecules Center, Peking University, Beijing 100871, P.R. China

SUMMARY

N^6-methyladenosine (m^6A) is the most prevalent internal modification of messenger RNA (mRNA) in higher eukaryotes. Here we report ALKBH5 as another mammalian demethylase that oxidatively reverses m^6A in mRNA in vitro and in vivo. This demethylation activity of ALKBH5 significantly affects mRNA export and RNA metabolism as well as the assembly of mRNA

*Correspondence: arne.klungland@rr-research.no (A.K.), ygyang@big.ac.cn (Y.-G.Y.), chuanhe@uchicago.edu (C.H.).
[11]These authors contributed equally to this work

SUPPLEMENTAL INFORMATION Supplemental Information includes six figures, six tables, and Supplemental Experimental Procedures and can be found with this article online at http://dx.doi.org/10.1016/j.molcel.2012.10.015.

ACCESSION NUMBERS The GEO accession number for the RNA-seq data reported in this paper is GSE40132.

processing factors in nuclear speckles. *Alkbh5*-deficient male mice have increased m^6A in mRNA and are characterized by impaired fertility resulting from apoptosis that affects meiotic metaphase-stage spermatocytes. In accordance with this defect, we have identified in mouse testes 1,551 differentially expressed genes that cover broad functional categories and include spermatogenesis-related mRNAs involved in the p53 functional interaction network. The discovery of this RNA demethylase strongly suggests that the reversible m^6A modification has fundamental and broad functions in mammalian cells.

INTRODUCTION

Cellular RNAs such as mRNA, tRNA, rRNA, and snRNA have long been known to contain more than 100 structurally distinct posttranscriptional modifications (Cantara et al., 2011; Globisch et al., 2011). We speculate that some of these modifications could be dynamic and might even have regulatory roles analogous to those of protein and DNA modifications (He, 2010). The m^6A modification is of great interest because it is the most abundant modification in mammalian mRNA (Bokar, 2005).

While the m^6A base modification in DNA is a known epigenetic marker that influences many fundamental cell processes in prokaryotes, there is no direct evidence that m^6A exists in the DNA of higher eukaryotes. However, this modification is ubiquitous in the mRNA of eukaryotes and of viruses that replicate inside host nuclei; the modification also plays an important role in meiosis and sporulation in yeast (Bokar, 2005; Shah and Clancy, 1992). m^6A is the most prevalent modification in mammalian mRNA, while also existing in tRNA (Saneyoshi et al., 1969) and rRNA (Iwanami and Brown, 1968).

In mammals, each mRNA contains, on average, 3–5 m^6A modifications within a consensus sequence previously revealed as Pu[G > A]m^6AC[A/C/U] (Bodi et al., 2010; Dominissini et al., 2012; Bokar, 2005; Harper et al., 1990; Meyer et al., 2012); experimental results indicate that only a portion of the putative methylation consensus sites in mammalian mRNA contain m^6A modifications (Kane and Beemon, 1985). m^6A on mRNA is believed to be installed by a methyltransferase complex, which has yet to be fully characterized. Biochemical studies have suggested that the methyltransferase exhibits sequence specificity to GAC and AAC, which accounts for the m^6A-containing consensus sequence (Nichols and Welder, 1981; Schibler et al., 1977; Wei et al., 1976). The importance of m^6A in mRNA has been shown through the knockdown of MT-A70—a key component of the proposed methyltransferase complex (Bokar et al., 1997)—in HeLa and plant cells, which led to apoptosis in HeLa cells and arrested development in plants (Bokar, 2005; Zhong et al., 2008). Previous studies utilizing methylation inhibitors have pointed to potential roles of m^6A in RNA processing events and mRNA transport in mammalian cells (Camper et al., 1984; Finkel and Groner, 1983). However, the exact functions of m^6A in mRNA have yet to be revealed.

Methylation on cytosines of mammalian DNA and histone residues are known to regulate gene expression (Gal-Yam et al., 2008; Gardner et al., 2011; Jaenisch and Bird, 2003). The recent discoveries of demethylases that actively remove methylations in DNA and histones provide a dynamic picture of mammalian gene expression regulation through reversible methylation (He et al., 2011; Ito et al., 2011; Shi et al., 2004; Tahiliani et al., 2009; Tsukada et al., 2006). We have proposed that analogous dynamic RNA modifications may exist and play significant roles in regulating gene expression (He, 2010). Indeed, we discovered that the human obesity-associated FTO protein (Fischer et al., 2009; Frayling et al., 2007; Gerken et al., 2007; Scott et al., 2007) is an RNA demethylase that oxidatively removes the m^6A modification in mRNA (Jia et al., 2011). Since our discovery, two groups have recently reported a strategy of m^6A-seq for profiling m^6A on RNA and revealed relatively conserved

RNA methylomes for human and mouse cells (Dominissini et al., 2012; Meyer et al., 2012). The involvement of m^6A in gene regulation has also been proposed.

FTO belongs to the AlkB family of nonheme Fe(II)/α-ketoglutarate (α-KG)-dependent dioxygenases, which catalyze a wide range of biological oxidations (Dango et al., 2011; Duncan et al., 2002; Falnes et al., 2002; Fu et al., 2010; Gerken et al., 2007; Sedgwick, 2004; Trewick et al., 2002; van den Born et al., 2011; Yi et al., 2010). The discovery of FTO as an RNA demethylase raises questions regarding how general such a process could be and whether m^6A plays roles in other biological processes. We present here ALKBH5 as another mammalian RNA demethylase that catalyzes the removal of the m^6A modification on nuclear RNA (mostly mRNA) in vitro and in vivo. Its demethylation activity affects nuclear RNA export and metabolism, gene expression, and mouse fertility, supporting the broad biological roles of the reversible m^6A modification on RNA.

RESULTS AND DISCUSSION

ALKBH5 Catalyzes Demethylation of m^6A-Containing RNA

Nine protein homologs were identified within the AlkB family. We therefore asked if there are RNA demethylases among these proteins other than FTO. We biochemically tested the demethylation activity of recombinant AlkB human homologs toward single-stranded RNA (ssRNA) and single-stranded DNA (ssDNA) substrates with site-specifically incorporated m^6A. The nucleic acid substrate was incubated with an equal amount of each recombinant protein at pH 7.5 and 16° C overnight, followed by complete digestion to single nucleoside by nuclease P1 and alkaline phosphatase, and subsequently analyzed by HPLC (Figures S1A and S1B available online). To our delight, we found that recombinant ALKBH5 (Figure S1C) can completely demethylate m^6A in the RNA/DNA substrates under these conditions (Figures 1A and 1B). Mass spectrometry was employed to confirm these results. An 8-mer ssDNA containing m^6A was treated with 30 mol% ALKBH5 at pH 7.5 for 30 min and then analyzed by MALDI-TOF/TOF. A 14 Da loss in substrate mass further verified the demethylation activity of ALKBH5 toward m^6A (Figure S1D).

Although recombinant human ALKBH5 has recently been reported to mediate the decarboxylation of α-KG and as a potential mRNA-binding protein (Baltz et al., 2012; Thalhammer et al., 2011), its exact function has never been revealed. To link the observed demethylation activity to the iron center, two mutant ALKBH5 proteins with the iron ligand residues H204 or H266 substituted to Ala were constructed (Figure S1C). The activity of the ALKBH5 mutant H266A was significantly compromised, while the other mutant, ALKBH5 H204A, completely lost its demethylation activity (Figure 1C), which is consistent with the mechanism of oxidative demethylation catalyzed by the iron center.

In order to compare the demethylation activity of ALKBH5 with that of the previously published FTO protein, we investigated the enzymatic kinetics of the ALKBH5-mediated demethylation reaction. The results showed that ALKBH5 demethylates the m^6A-containing ssRNA with an activity comparable to FTO (Jia et al., 2011) (Figure 1D and Table S1).

We further investigated the demethylation activity of ALKBH5 toward various m^6A-containing synthetic oligonucleotides. These oligonucleotides were incubated with ALKBH5 at room temperature for 2.5 hr to monitor and compare reaction rates using LC-MS/MS (Figures S1E and S1F). We first tested m^6A-containing ssRNA and ssDNA with the same sequence. Demethylation yields of ~39% for ssRNA and ~45% for ssDNA were observed. We tested a known sequenceof cellular bovine prolactin (bPRL) mRNA, which forms a stem loop secondary structure with m^6A in the loop (Bokar, 2005), under the same reaction conditions with an ~23% demethylation yield observed, which indicates no

preference of ALKBH5 toward m^6A in a loop. ALKBH5 strongly prefers single-stranded substrates, as it exhibits an almost unnoticeable demethylation activity toward m^6A in a 26-mer double-stranded RNA (dsRNA; a 26-mer sequence was used to prevent potential reversible annealing at room temperature). Most m^6A modifications in mammalian mRNA exist in a consensus sequence of (Pu[G > A]m^6AC[A/C/U]). We therefore synthesized and tested 15-mer ssRNAs with the currently known consensus sequences of (GGm^{6}ACU)/(CAm^{6}ACA) (Dominissini et al., 2012; Meyer et al., 2012) and a random sequence of (CUm^{6}AUU). While ALKBH5 shows similar activity toward these two consensus sequences (~40%), a reduced demethylation yield of ~20% was observed toward the nonconsensus sequence under the same conditions (Figure S1G), suggesting that ALKBH5 may have a sequence preference in demethylation.

m^6A in mRNA Is a Physiologically Relevant Substrate of ALKBH5

Since m^6A has not been identified in genomic DNA in mammals (see also our results from mouse tissues later on), the most likely cellular substrates of ALKBH5 are m^6A modifications of mRNA or other nuclear RNAs. Given that m^6A is one of the most common modifications on mRNA and our discovery of FTO as an m^6A demethylase (Jia et al., 2011), we asked if ALKBH5 could demethylate m^6A on mRNA inside mammalian cells. To verify the observed demethylation activity inside cells, ALKBH5 was knocked down by siRNA in HeLa cells, and the relative level of m^6A in total mRNA was quantified by LC-MS/MS following the published procedure (Jia et al., 2011). An ~9% increase of the m^6A level in total mRNA was consistently observed in repeated experiments following a 48 hr knockdown (Figure 2A). ALKBH5 was also overexpressed in HeLa cells, which led to a significant decrease of the m^6A level in total mRNA by ~29% after 24 hr (Figure 2A). These data confirmed that m^6A in mRNA is a physiologically relevant substrate of ALKBH5 inside cells. As a control, we also monitored the m^6A level of ribosomal RNA (rRNA) in HeLa cells with and without ALKBH5 knockdown. We failed to observe a statistically significant increase of m^6A in rRNA within the detection limit of the current LC-MS/MS method (Figure S2A). Although we cannot rule out m^6A on rRNA as a potential substrate of ALKBH5, it is clear that m^6A on mRNA is the major substrate of ALKBH5. Considering that over 10,000 m^6A sites were identified in more than 7,000 human mRNAs (Dominissini et al., 2012; Meyer et al., 2012), an ~10%–20% change of m^6A level could result in a profound impact if the modification does play a regulatory role.

A very recent study characterizing the mRNA-bound proteome has revealed close to 800 potential mRNA-binding proteins using quantitative proteomics that include ALKBH5 (Baltz et al., 2012). Although no function was reported, the results support our functional characterization of ALKBH5 as an mRNA demethylase. We selected a few mRNAs, shown to be potentially bound by ALKBH5 (Baltz et al., 2012) and contain m^6A sites, with *GAPDH* (Glyceraldehyde 3-phosphate dehydrogenase) as an unbound negative control that does not contain known m^6A sites (Dominissini et al., 2012; Meyer et al., 2012). We performed immunoprecipitation of isolated HeLa mRNA, separating it into an m^6A antibody-bound fraction and an m^6A-depleted fraction. The relative abundance of individually selected mRNA in these two fractions was quantified by RT-qPCR following a published procedure (Bodi et al., 2010) (Figure S2B). Four out of six tested mRNAs were enriched in the m^6A antibody-bound fraction in control samples (without ALKBH5 knockdown), confirming the presence of m^6A sites on these transcripts. All of the selected mRNAs (except *GAPDH*) showed increased enrichment in the m^6A antibody-bound fraction when ALKBH5 was knocked down, thus indicating that m^6A sites on these potential ALKBH5-bound mRNAs are likely the direct substrates subject to ALKBH5-catalyzed demethylation. This observation at the individual mRNA level further supports ALKBH5 as an RNA demethylase.

ALKBH5 Colocalizes with Nuclear Speckles and Influences mRNA Processing Factors' Assembly/Modification

MT-A70, the identified subunit of the m^6A methyltransferase that introduces methyl group to adenosine on mRNA has been shown to colocalize with nuclear speckles (Bokar, 2005). It is possible that m^6A on mRNA is dynamically regulated by enzymes with opposing activities to affect mRNA metabolism. Indirect immunofluorescence analysis was employed to characterize the cellular localization of ALKBH5 in HeLa cells. ALKBH5 has been shown to colocalize well with mRNA-processing factors that include phosphorylated SC35 (SC35-pi) (serine/arginine-rich splicing factor 2), SM (Smith antigen), and ASF/SF2 (alternative splicing factor/splicing factor 2) in nuclear speckles (Figures 2B and S2C). SC35 associates with nuclear speckles through protein-protein interaction, and thus its localization is not affected by RNase treatment, whereas SM is an RNA-binding protein, and its localization in nuclear speckles is sensitive to RNase treatment (Ricciardi et al., 2009). ALKBH5 exhibits a diffused nucleoplasmic pattern with intense granule-like foci in an RNase A-sensitive manner similar to SM. Unlike SC35, after RNase A treatment, signals of the ALKBH5 granule-like foci decreased notably, suggesting cellular interactions between ALKBH5 and nuclear RNA (Figure 2B).

When ALKBH5 was knocked down in HeLa cells, we observed disappearance of SC35-pi staining (Figure 2C), suggesting association of ALKBH5 with certain mRNA-processing factors in nuclear speckles. To investigate if the diminished staining caused by ALKBH5 depletion could be attributed to the demethylation activity of ALKBH5, WT ALKBH5 and the demethylation-inactive mutant ALKBH5 H204A were subcloned into the pEGFP-C1b vector. Complementation of the knockdown experiment with WT ALKBH5 restored signals of SC35-pi staining, whereas expression of the inactive mutant ALKBH5 failed to do so (Figure 2C), thus indicating that the demethylation activity of ALKBH5 is important to the proper assembly/modification of certain mRNA processing factors.

ALKBH5 Affects mRNA Export and RNA Metabolism

To investigate the effects of ALKBH5 on RNA metabolism, subcellular distribution of nascent RNA was examined by 5-Bromouridine (BrU)-incorporation followed by immunofluorescence analysis. Intriguingly, cytoplasmic RNA level was significantly increased in ALKBH5-deficient cells as a result of the accelerated nuclear RNA export (Figure S3A). Since we have shown that mRNA is the major substrate of ALKBH5, it is very likely that mRNA export is altered in ALKBH5-deficient cells; also note that rRNA in the nucleolus typically cannot be well imaged in this specific assay as a result of the intact and antibody-inaccessible structure of the nucleoli (Haukenes and Kalland, 1998).

To confirm our speculation, we applied the fluorescent in situ hybridization (FISH) approach to monitor mRNA and rRNA export. Using an oligo$(dT)_{50}$-digoxigenin probe for the poly(A) tail, we observed that mRNA is predominantly localized in the cytoplasm in ALKBH5-deficient cells in contrast to its strong nuclear accumulation in cells with ALKBH5 (Figure 3A). Quantitative analysis further confirmed a dramatic shift in the ratio of nuclear mRNA to cytoplasmic mRNA when ALKBH5 was knocked down (Figure S3B). Meanwhile, the rRNA-FISH experiment showed that the majority of rRNA was already present in the cytoplasm and the depletion of ALKBH5 does not noticeably perturb rRNA distribution between the cytoplasm, nucleus, and nucleolus (Figure S3C). In addition, only overexpression of the WT, demethylation-active ALKBH5—but neither the empty vector nor the catalytic inactive mutant H204A—could rescue this accelerated mRNA export in both BrU and poly(A)-RNA-FISH assays (Figures S3A and 3A, right panels), which indicates that ALKBH5 mainly affects mRNA export through its demethylation activity.

It is known that different export pathways are utilized by different RNAs (Köhler and Hurt, 2007). The TAP-p15 complex, together with other RNA-binding adaptor proteins, functions as the general mRNA-export cargo to transport mRNA through the nuclear pore complex. We have noticed that ALKBH5 colocalizes with ASF/SF2, and these SR proteins are known to switch from splicing factors to export adaptor proteins through changing their phosphorylation status (Gilbert and Guthrie, 2004). Hyperphosphorylated ASF/SF2 is involved in pre-mRNA splicing while hypophosphorylated ASF/SF2 bridges the interaction of the TAP-p15 complex and mRNA cargo to facilitate mRNA export (Li and Manley, 2005; Michlewski et al., 2008). Interestingly, the staining of ASF/SF2 was dramatically diminished in ALKBH5-deficient HeLa cells (Figure 3B). The signal could be efficiently rescued by complementation with WT ALKBH5, but not with the inactive mutant H204A, indicating that the function of ASF/SF2 is likely affected by ALKBH5 in a demethylation-dependent manner. Western blot analysis verified the decreased level of phosphorylated ASF/SF2 when ALKBH5 was knocked down (Figure S3D).

We further discovered that SRPK1, one of the main kinases responsible for the phosphorylation of ASF/SF2, was relocalized from nucleic locations to dot-like cytoplasmic sites in ALKBH5-deficient cells (Figure 3C). Only complementation with the WT ALKBH5, but not the inactive mutant H204A, could rescue its native localization. SRPK1 catalyzes phosphorylation of mRNA-processing factors including ASF/SF2 (Giannakouros et al., 2011). The altered subcellular localization of SRPK1 in the ALKBH5-deficient cells may partially account for the changed ASF/SF2 phosphorylation status. Given the importance of the demethylation activity of ALKBH5 on the cellular locations of some of these mRNA-processing factors, it is likely that the m^6A methylation status of mRNA transcripts targeted by ALKBH5 influences the cellular dynamics of their processing factors. The detailed pathways and mechanism can be complex and should be further investigated in the future.

To further explore the roles of ALKBH5 on RNA metabolism, nascent RNA synthesis was monitored by using 5-ethynyl uridine (EU) labeling followed by flow cytometry analysis. When we knocked down ALKBH5 in HeLa cells, we observed that ALKBH5 deficiency increased the rate of nascent RNA synthesis (Figure S4A) and slightly reduced global RNA stability (Figure S4B), suggesting complex roles played by ALKBH5 in RNA metabolism. Indeed, transcriptome analysis in ALKBH5-deficient HeLa cells compared to control cells revealed 2,740 differentially expressed genes (DEGs) in total, with 1,158 genes differentially expressed at the gene level (Table S2A) and the remaining 3,356 at isoform level (Table S2B). Based on Gene Ontology (GO) analysis, 492 of these DEGs were enriched in functional pathways related to RNA metabolic processes (Figure 4 and Table S3), consistent with the functional analysis performed on the published PAR-CLIP result of ALKBH5 in HEK293 cells (Baltz et al., 2012) that RNA metabolism is one of the most enriched functional pathways (Figure S4C and Table S4), therefore supporting the broad impact of ALKBH5 on RNA metabolism and other cellular functions. Although EU chemically labels both rRNA and mRNA, our transcriptome analysis (Table S3) indicates that rRNA biogenesis, processing, and other metabolic processes ($p > 0.99$) have a low probability of being affected. rRNA may be perturbed indirectly through other pathways affected by ALKBH5.

Alkbh5 Deficiency Leads to Compromised Spermatogenesis in Mice

The impact on nuclear RNA processing and metabolism observed in cultured mammalian cells suggests that ALKBH5 may affect biological processes in animals. We examined the expression levels of *Alkbh5* mRNA in multiple mouse organs by RT-qPCR. *Alkbh5* mRNA was detected in all organs studied, with the highest expression found in testes (Figure 5A). To further examine the function of this gene, a targeted deletion of *Alkbh5* in the mice was

created by removing the transcription start site and exon 1 of the genomic *Alkbh5* locus (Figure 5B). *Alkbh5*$^{-/-}$ mice were viable, anatomically normal, and reached adulthood. However, when *Alkbh5*$^{-/-}$ and heterozygous *Alkbh5*$^{+/-}$ were crossed in combinations, we observed a remarkably low success rate of breeding (Figure S5A). These results, combined with the high expression level of *Alkbh5* in testes, directed our attention to spermatogenesis.

Testes of *Alkbh5*$^{-/-}$ mice were found to be significantly smaller than those of WT littermates (Figure 5C). Comparative histological analysis of testis sections revealed aberrant tubular architecture and size in *Alkbh5*-deficient mice (Figure 5D). The number of spermatozoa released from *Alkbh5*$^{-/-}$-dissected cauda epididymes was dramatically reduced, and the spermatozoa were morphologically abnormal with greatly compromised motility (Figures 5E, 5F, and S5B). RNA in situ hybridization confirmed that there was no detectable *Alkbh5* expression in the adult testes of *Alkbh5*-deficient mice, whereas in WT littermates, it showed that *Alkbh5* expression in the testis is highly specific to primary spermatocytes (Figure S5C). Quantification of the relative density of germ cells in stage VII seminiferous tubuli demonstrated a significantly reduced number of pachytene spermatocytes and round spermatids in *Alkbh5*-deficient mice (Figure S5D). The increase in the primary to secondary spermatocyte ratio was further visualized by immunofluorescence staining (Figure 5G), which strongly indicates spermatogenic maturation arrest and failure to enter and proceed through spermiogenesis.

We further showed by TUNEL staining that massive cell death through apoptosis occurs in *Alkbh5*-deficient testes (Figures 5H and S5E). The timing of apoptosis was quantified according to cell type and spermatogenic stage, which revealed increased apoptosis at stage XI and XII spermatocytes and a metaphase arrest. Taken together, mice deficient in *Alkbh5* have compromised spermatogenesis, which likely results in apoptosis of pachytene and metaphase-stage spermatocytes and aberrant spermiogenesis. A low number of spermatozoa with poor quality were generated as a result of this defect, which explains the impaired fertility in the male mice.

Increased m^{6}A Levels in Total mRNA Isolated from *Alkbh5*-Deficient Mouse Organs

To investigate the nucleic acid substrate of Alkbh5 in mouse tissues, we evaluated the potential presence of m^{6}A in DNA. Genomic DNA isolated from the testes, lungs, and brains of WT mice and *Alkbh5*-deficient mice was assessed using LCMS/MS. We failed to detect m^{6}A in genomic DNA samples from any of these organs within the detection limit (less than 1 m^{6}A in every 6×10^6 nucleotides) (Figure S6A). To confirm the role of Alkbh5 as an RNA demethylase in mouse tissues as we have shown in cell lines, we isolated mRNA from purified testicular cells contained within seminiferous tubuli where meiosis takes place and gametes are created (further referred to as testicular cells) as well as from the lungs, the organ with the second highest *Alkbh5* expression. We compared the m^{6}A level of samples from WT mice with *Alkbh5*-deficient mice. Indeed, we observed a statistically significant increase of the m^{6}A level in samples from *Alkbh5*-deficient mice (Figures 6A and S6B), which strongly supports that ALKBH5 is an RNA demethylase working on mRNA in mammals.

Spermatogenesis is a complex, highly regulated process with many unique features when compared to other somatic cellular pathways. For instance, nuclear transcription is stalled during spermatogenesis, and hundreds of sperm proteins required for the process are synthesized from stored mRNAs (Goldberg, 2000). The stability and transportation of these mRNAs are thus critical for proper cellular function. Therefore, a deficiency of *Alkbh5*, which leads to abnormal RNA metabolism as we showed in cell lines, could impact cytoplasmic levels of key mRNAs required for proper spermatogenic maturation, which could explain the observed phenotype.

Expression of Spermatogenesis Genes Is Affected by *Alkbh5* Deficiency

We then asked how the deficiency of *Alkbh5* could lead to testicular dysfunction resulting in compromised spermatogenesis. A comprehensive understanding of gene expression alterations would help us to address this question. Therefore, we sequenced and compared the transcriptomes of testicular cells from the WT mice and *Alkbh5*-deficient mice to identify genes that could be involved in the observed spermatogenesis phenotype. A total of 1,551 genes showed a significant difference in expression, with 646 genes differentially expressed at the gene level (Table S5A) and 1,752 differentially expressed isoforms (Table S5B).

The limited amounts of RNA yielded from a low number of testicular cells that can be purified from the defected testes and the pioneering stage of establishing spermatogonial stem cell lines from mice (Sato et al., 2011) made extensive validation of these genes difficult at this stage. We therefore looked into published studies for mechanistic insights underlying the impaired spermatogenesis. We sorted the differentially expressed transcripts with reference to a compiled data set of reported spermatogenesis/infertility-related genes (Ashburner et al., 2000; Consortium, 2012; He et al., 2007; Pang et al., 2006; Rockett et al., 2004; Rossi et al., 2004; Safran et al., 2010; Shaha et al., 2010). Out of 1,551 transcripts, 127 were sorted as previously reported spermatogenesis-related (Figure S6B and Table S5C). It is very likely that other genes identified in our study may have hitherto unknown roles related to mammalian spermatogenesis, but they could not be assigned to the compiled data set due to lack of literature reports. Our data may thus include other spermatogenesis-related genes not listed among the assigned 127 genes and provide a useful reference resource for future studies. Functional interaction network analysis revealed that 78 out of the 127 genes belong to the p53 functional interaction network (Figure 6B), which is consistent with the induction of apoptosis and aberrant differentiation observed in the *Alkbh5*-deficient mouse testes. As expected, in addition to apoptosis, GO analysis of all of the 1,551 genes revealed diverse functions of Alkbh5, for example chromatin organization, signaling transduction, and RNA metabolism (Table S6), indicating a potential broad regulatory function of Alkbh5.

We next selected 31 genes based on transcriptome analysis for validation. Although there were differences for some genes in the level of fold change between the RNA-seq data and the RT-qPCR validation, 18 phenotypically relevant genes all exhibited changes in the same direction (Figure 6C), suggesting a significant impact of Alkbh5 on these mRNAs. *Eif4g1* is targeted for proteolytic cleavage during inhibition of translation in apoptotic cells (Marissen and Lloyd, 1998); *Fos* exerts a regulatory role in spermatogenesis, and its decreased expression is implicated to result in reduction in germ cell number, differentiation, and fertility (Shalini and Bansal, 2006); *Spata3* is involved in spermatocyte development (Li et al., 2009); *Fgfr1*-deficient mice are subfertile, and this gene is required for normal spermatogenesis (Cotton et al., 2006); and *Otof*, a gene conserved from nematodes to mammals, is required for vesicle fusion in spermatides during spermiogenesis in *Caenorhabditis elegans* (Achanzar and Ward, 1997). Moreover, we observed differential expression of *Dnmt1* (DNA methyltransferase 1) and *Uhrf1* (ubiquitin-like with PHD and RING finger domains 1), both playing key roles in determining genomic 5-methylcytosine methylation patterns in spermatocyte development (Sharif et al., 2007). Constitutive exons presented in all four splice variants of *Dnmt1* (*Dnmt1 all*) showed a trend of increased expression, whereas the expression of the pachytene spermatocyte-specific *Dnmt1* (*Dnmt1 t*) was reduced in *Alkbh5*-deficient testicular cells. Constitutive exons of the four *Uhfr1* splice variants (*Uhfr1 all*) as well as the exon unique to variant 2 and 4 (*Uhfr1 2+4*) showed clearly reduced expression, although the effect on the constitutive exons was more pronounced, which was likely contributed by the effect on variant 1 and/or 3. These examples may suggest that *Alkbh5* deficiency could affect splice variants. RT-qPCR of another 13 genes

not connected to the phenotype further validated the RNA-seq result (Figure S6D). Therefore, our results indicate significant alterations of key genes involved in spermatogenesis, which accounts for the observed phenotype of the *Alkbh5*$^{-/-}$ mouse. Since Alkbh5 affects many RNA substrates, other pathways may also contribute to the impaired fertility, and the global effect could be complex.

In summary, we report ALKBH5 as another mammalian m^{6}A RNA demethylase both in vitro and in vivo. Deficiency of ALKBH5 leads to increased m^{6}A in total mRNA as well as individual mRNA isolated from cells. ALKBH5 and its demethylation activity play important roles in mRNA export as well as roles in the association of the nuclear speckle proteins and RNA metabolism. In addition, increased m^{6}A was observed in total mRNA samples isolated from tissues from *Alkbh5*$^{-/-}$ mice compared to those from the WT mice, further confirming ALKBH5 as an RNA demethylase. The *Alkbh5* deficiency leads to aberrant spermatogenesis and apoptosis in mouse testes. Transcriptome analysis revealed differentially expressed genes associated with spermatogenesis and the p53 functional interaction network, in line with the impaired fertility observed for the *Alkbh5*$^{-/-}$ mouse. Although spermatogenesis is a noticeable defect associated with the *Alkbh5*$^{-/-}$ mouse, our transcriptome analysis of Alkbh5 and cell-based studies indicate that this protein could impact many other biological processes through the demethylation of m^{6}A on RNA. Thus, the discovery and characterization of this second RNA demethylase, in addition to FTO, have significant implications; it shows that the reversible m^{6}A modification in mammalian mRNA plays broad and critical roles in fundamental biological processes. Reversible RNA modifications may indeed exert an additional layer of biological regulation on multifaceted life processes similar to those observed on DNA and histones (He, 2010).

EXPERIMENTAL PROCEDURES

Cloning and Expression of ALKBH5

The human ALKBH5 (GenBank Accession number NP_060228.3) with deletion of the amino-terminal 66 amino acids was subcloned into a pMCSG19 vector by ligation-independent cloning (LIC) to generate the plasmid pMCSG19-His-*ALKBH5*. ALKBH5 and mutants were expressed in the BL21 (DE3) *E. coli* strain and purified for activity characterization.

RNA FISH

Poly(A)-tailed RNA FISH was performed using the hybridization mixture containing digoxigenin-tagged oligo(dT)$_{50}$ probes (Huang et al., 1994). rRNA FISH was performed using a digoxigenin-tagged probe targeting nucleotide +4271/+4379 of human 18S rRNA, as described (Dundr and Olson, 1998). Immunofluorescence assay was performed after in situ hybridization by using anti-digoxigenin and anti-ALKBH5 antibodies.

Alkbh5 Gene Targeting

In brief, the genomic *Alkbh5* locus was cloned and LoxP sites inserted upstream of exon 1 and in intron 1. A neo cassette flanked by Frt sites was inserted just upstream of the LoxP sequence in intron 1. Neo-resistant recombinant ESCs were analyzed for correct 3′ and 5′ targeting through hybridization by standard protocols, and we identified seven correctly targeted clones. Following ESC cell injection, several high-percentage chimera males were born. These were bred with Cre-expressing mice, and Cre-mediated excision of *Alkbh5* exon 1 was tested in 26 agouti F1 pups. Two animals tested positive for the excised allele. These two mice, heterozygous for the constitutive allele (*Alkbh5*$^{+/-}$), were analyzed by Southern blot analysis and used for further breeding to generate *Alkbh5*$^{-/-}$ mice.

All animal experiments were approved by the Section for Comparative Medicine at Oslo University Hospital and by the Norwegian Animal Research Authority. National laws and Federation for Laboratory Animal Science Associations (FELASA) regulations were complied with and followed. Additional details, as well as graphical descriptions, can be obtained from the corresponding authors upon request.

RNA-Seq

Total RNA was isolated from siRNA-treated HeLa cells or mouse testicular cells using RNAzol (Molecular Research Center, Inc.). Poly(A) RNA from 1 μg total RNA was used to generate the cDNA library according to TruSeq RNA Sample Prep Kit protocol, which was then sequenced using the HiSeq 2000 system (Illumina). Human and mouse RNA-seq reads were mapped to the Human (hg19) and Mouse (mm9) genomes, respectively, using TopHat (version 2.0.0) (Trapnell et al., 2009). At most, two mismatches were allowed. Only the uniquely mapped reads were kept for the subsequent analysis. The gene differential expression analysis was performed using Cuffdiff software (version 2.0.0) (Trapnell et al., 2010) with default parameters.

Supplementary Material

Refer to Web version on PubMed Central for supplementary material.

Acknowledgments

This study was supported by National Institutes of Health (GM071440 to C.H.), the China 973 program (2011CB510103 to Y.-G.Y.), the CAS Innovation Program for Young Scientists (Y.N.), the CAS “100-talents” Professor Program (Y.-G.Y.), the National Natural Science Foundation of China (30900724 and 81071648 to Y.N.), the CAS Senior Foreign Research Fellow Award (2011T1S21 to A.K.), the China 973 (2011CB809103 to C.H.), the Norwegian Cancer Society, and the FRIBIO and FUGE programs in the Research Council of Norway. We thank Dr. T. Lindahl for providing reagents; Dr. P. Reddi for discussion on spermatogenesis; BIOPIC for RNA-seq; D.M. Tian, S. Xiang, T.T. Chen, and N. Wu for bioinformatics analysis; G.F. Lien, L. Ellevåg, H. Wiksen, K. Schramm, and E.K.K. Henriksen for skillful technical help; and S.F. Reichard, MA for editing the manuscript.

REFERENCES

Achanzar WE, Ward S. A nematode gene required for sperm vesicle fusion. J. Cell Sci. 1997; 110:1073–1081. [PubMed: 9175703]

Ashburner M, Ball CA, Blake JA, Botstein D, Butler H, Cherry JM, Davis AP, Dolinski K, Dwight SS, Eppig JT, et al. The Gene Ontology Consortium. Gene ontology: tool for the unification of biology. Nat. Genet. 2000; 25:25–29. [PubMed: 10802651]

Baltz AG, Munschauer M, Schwanhaüsser B, Vasile A, Murakawa Y, Schueler M, Youngs N, Penfold-Brown D, Drew K, Milek M, et al. The mRNA-bound proteome and its global occupancy profile on protein-coding transcripts. Mol. Cell. 2012; 46:674–690. [PubMed: 22681889]

Bodi Z, Button JD, Grierson D, Fray RG. Yeast targets for mRNA methylation. Nucleic Acids Res. 2010; 38:5327–5335. [PubMed: 20421205]

Bokar, JA. Fine-Tuning of RNA Functions by Modification and Editing. Grosjean, H., editor. Vol. Volume 12. Springer; New York: 2005. p. 141-177.

Bokar JA, Shambaugh ME, Polayes D, Matera AG, Rottman FM. Purification and cDNA cloning of the AdoMet-binding subunit of the human mRNA (N^6-adenosine)-methyltransferase. RNA. 1997; 3:1233–1247. [PubMed: 9409616]

Camper SA, Albers RJ, Coward JK, Rottman FM. Effect of undermethylation on mRNA cytoplasmic appearance and half-life. Mol. Cell. Biol. 1984; 4:538–543. [PubMed: 6201720]

Cantara WA, Crain PF, Rozenski J, McCloskey JA, Harris KA, Zhang X, Vendeix FA, Fabris D, Agris PF. The RNA Modification Database, RNAMDB: 2011 update. Nucleic Acids Res. 2011; 39(Database issue):D195–D201. [PubMed: 21071406]

Consortium TU, UniProt Consortium. Reorganizing the protein space at the Universal Protein Resource (UniProt). Nucleic Acids Res. 2012; 40(Database issue):D71–D75. [PubMed: 22102590]

Cotton L, Gibbs GM, Sanchez-Partida LG, Morrison JR, de Kretser DM, O'Bryan MK. FGFR-1 [corrected] signaling is involved in spermiogenesis and sperm capacitation. J. Cell Sci. 2006; 119:75–84. [PubMed: 16352663]

Dango S, Mosammaparast N, Sowa ME, Xiong LJ, Wu F, Park K, Rubin M, Gygi S, Harper JW, Shi Y. DNA unwinding by ASCC3 helicase is coupled to ALKBH3-dependent DNA alkylation repair and cancer cell proliferation. Mol. Cell. 2011; 44:373–384. [PubMed: 22055184]

Dominissini D, Moshitch-Moshkovitz S, Schwartz S, Salmon-Divon M, Ungar L, Osenberg S, Cesarkas K, Jacob-Hirsch J, Amariglio N, Kupiec M, et al. Topology of the human and mouse m^6A RNA methylomes revealed by m^6A-seq. Nature. 2012; 485:201–206. [PubMed: 22575960]

Duncan T, Trewick SC, Koivisto P, Bates PA, Lindahl T, Sedgwick B. Reversal of DNA alkylation damage by two human dioxygenases. Proc. Natl. Acad. Sci. USA. 2002; 99:16660–16665. [PubMed: 12486230]

Dundr M, Olson MOJ. Partially processed pre-rRNA is preserved in association with processing components in nucleolus-derived foci during mitosis. Mol. Biol. Cell. 1998; 9:2407–2422. [PubMed: 9725903]

Falnes PO, Johansen RF, Seeberg E. AlkB-mediated oxidative demethylation reverses DNA damage in *Escherichia coli*. Nature. 2002; 419:178–182. [PubMed: 12226668]

Finkel D, Groner Y. Methylations of adenosine residues (m^6A) in pre-mRNA are important for formation of late simian virus 40 mRNAs. Virology. 1983; 131:409–425. [PubMed: 6318439]

Fischer J, Koch L, Emmerling C, Vierkotten J, Peters T, Brüning JC, Rüther U. Inactivation of the *Fto* gene protects from obesity. Nature. 2009; 458:894–898. [PubMed: 19234441]

Frayling TM, Timpson NJ, Weedon MN, Zeggini E, Freathy RM, Lindgren CM, Perry JRB, Elliott KS, Lango H, Rayner NW, et al. A common variant in the *FTO* gene is associated with body mass index and predisposes to childhood and adult obesity. Science. 2007; 316:889–894. [PubMed: 17434869]

Fu Y, Dai Q, Zhang W, Ren J, Pan T, He C. The AlkB domain of mammalian ABH8 catalyzes hydroxylation of 5-methoxycarbonylmethyluridine at the wobble position of tRNA. Angew. Chem. Int. Ed. Engl. 2010; 49:8885–8888. [PubMed: 20583019]

Gal-Yam EN, Saito Y, Egger G, Jones PA. Cancer epigenetics: modifications, screening, and therapy. Annu. Rev. Med. 2008; 59:267–280. [PubMed: 17937590]

Gardner KE, Allis CD, Strahl BD. Operating on chromatin, a colorful language where context matters. J. Mol. Biol. 2011; 409:36–46. [PubMed: 21272588]

Gerken T, Girard CA, Tung YCL, Webby CJ, Saudek V, Hewitson KS, Yeo GSH, McDonough MA, Cunliffe S, McNeill LA, et al. The obesity-associated *FTO* gene encodes a 2-oxoglutarate-dependent nucleic acid demethylase. Science. 2007; 318:1469–1472. [PubMed: 17991826]

Giannakouros T, Nikolakaki E, Mylonis I, Georgatsou E. Serine-arginine protein kinases: a small protein kinase family with a large cellular presence. FEBS J. 2011; 278:570–586. [PubMed: 21205200]

Gilbert W, Guthrie C. The Glc7p nuclear phosphatase promotes mRNA export by facilitating association of Mex67p with mRNA. Mol. Cell. 2004; 13:201–212. [PubMed: 14759366]

Globisch D, Pearson D, Hienzsch A, Brückl T, Wagner M, Thoma I, Thumbs P, Reiter V, Kneuttinger AC, Müller M, et al. Systems-based analysis of modified tRNA bases. Angew. Chem. Int. Ed. Engl. 2011; 50:9739–9742. [PubMed: 21882308]

Goldberg, E. The testis: from stem cell to sperm function. Springer; New York: 2000.

Harper JE, Miceli SM, Roberts RJ, Manley JL. Sequence specificity of the human mRNA N6-adenosine methylase *in vitro*. Nucleic Acids Res. 1990; 18:5735–5741. [PubMed: 2216767]

Haukenes G, Kalland K-H. Visualisation of ribosomal RNA (rRNA) synthesis in eukaryotic cells in culture. Methods Cell Sci. 1998; 19:295–302.

He C. Grand challenge commentary: RNA epigenetics? Nat. Chem. Biol. 2010; 6:863–865. [PubMed: 21079590]

He C, Zuo Z, Chen H, Zhang L, Zhou F, Cheng H, Zhou R. Genome-wide detection of testis- and testicular cancer-specific alternative splicing. Carcinogenesis. 2007; 28:2484–2490. [PubMed: 17724370]

He YF, Li BZ, Li Z, Liu P, Wang Y, Tang QY, Ding JP, Jia YY, Chen ZC, Li L, et al. Tet-mediated formation of 5-carboxylcytosine and its excision by TDG in mammalian DNA. Science. 2011; 333:1303–1307. [PubMed: 21817016]

Huang S, Deerinck TJ, Ellisman MH, Spector DL. *In vivo* analysis of the stability and transport of nuclear poly(A)$^+$ RNA. J. Cell Biol. 1994; 126:877–899. [PubMed: 7519622]

Ito S, Shen L, Dai Q, Wu SC, Collins LB, Swenberg JA, He C, Zhang Y. Tet proteins can convert 5-methylcytosine to 5-formylcytosine and 5-carboxylcytosine. Science. 2011; 333:1300–1303. [PubMed: 21778364]

Iwanami Y, Brown GM. Methylated bases of ribosomal ribonucleic acid from HeLa cells. Arch. Biochem. Biophys. 1968; 126:8–15. [PubMed: 5671075]

Jaenisch R, Bird A. Epigenetic regulation of gene expression: how the genome integrates intrinsic and environmental signals. Nat. Genet. 2003; 33(Suppl):245–254. [PubMed: 12610534]

Jia G, Fu Y, Zhao X, Dai Q, Zheng G, Yang Y, Yi C, Lindahl T, Pan T, Yang YG, He C. N6-methyladenosine in nuclear RNA is a major substrate of the obesity-associated FTO. Nat. Chem. Biol. 2011; 7:885–887. [PubMed: 22002720]

Kane SE, Beemon K. Precise localization of m^{6}A in Rous sarcoma virus RNA reveals clustering of methylation sites: implications for RNA processing. Mol. Cell. Biol. 1985; 5:2298–2306. [PubMed: 3016525]

Köhler A, Hurt E. Exporting RNA from the nucleus to the cytoplasm. Nat. Rev. Mol. Cell Biol. 2007; 8:761–773. [PubMed: 17786152]

Li X, Manley JL. Inactivation of the SR protein splicing factor ASF/SF2 results in genomic instability. Cell. 2005; 122:365–378. [PubMed: 16096057]

Li L, Liu G, Fu JJ, Li LY, Tan XJ, Yang S, Lu GX. Molecular cloning and characterization of a novel transcript variant of *Mtsarg1* gene. Mol. Biol. Rep. 2009; 36:1023–1032. [PubMed: 18551385]

Marissen WE, Lloyd RE. Eukaryotic translation initiation factor 4G is targeted for proteolytic cleavage by caspase 3 during inhibition of translation in apoptotic cells. Mol. Cell. Biol. 1998; 18:7565–7574. [PubMed: 9819442]

Meyer KD, Saletore Y, Zumbo P, Elemento O, Mason CE, Jaffrey SR. Comprehensive analysis of mRNA methylation reveals enrichment in 3′ UTRs and near stop codons. Cell. 2012; 149:1635–1646. [PubMed: 22608085]

Michlewski G, Sanford JR, Cáceres JF. The splicing factor SF2/ASF regulates translation initiation by enhancing phosphorylation of 4E-BP1. Mol. Cell. 2008; 30:179–189. [PubMed: 18439897]

Nichols JL, Welder L. Nucleotides adjacent to N^6-methyladenosine in maize poly(A)-containing RNA. Plant Sci. Lett. 1981; 21:75–81.

Pang AL, Johnson W, Ravindranath N, Dym M, Rennert OM, Chan WY. Expression profiling of purified male germ cells: stage-specific expression patterns related to meiosis and postmeiotic development. Physiol. Genomics. 2006; 24:75–85. [PubMed: 16291737]

Ricciardi S, Kilstrup-Nielsen C, Bienvenu T, Jacquette A, Landsberger N, Broccoli V. CDKL5 influences RNA splicing activity by its association to the nuclear speckle molecular machinery. Hum. Mol. Genet. 2009; 18:4590–4602. [PubMed: 19740913]

Rockett JC, Patrizio P, Schmid JE, Hecht NB, Dix DJ. Gene expression patterns associated with infertility in humans and rodent models. Mutat. Res. 2004; 549:225–240. [PubMed: 15120973]

Rossi P, Dolci S, Sette C, Capolunghi F, Pellegrini M, Loiarro M, Di Agostino S, Paronetto MP, Grimaldi P, Merico D, et al. Analysis of the gene expression profile of mouse male meiotic germ cells. Gene Expr. Patterns. 2004; 4:267–281. [PubMed: 15053975]

Safran, M.; Dalah, I.; Alexander, J.; Rosen, N.; Iny Stein, T.; Shmoish, M.; Nativ, N.; Bahir, I.; Doniger, T.; Krug, H., et al. GeneCards Version 3: the human gene integrator. Database; Oxford: 2010. p. baq0202010

Saneyoshi M, Harada F, Nishimura S. Isolation and characterization of N^6-methyladenosine from Escherichia coli valine transfer RNA. Biochim. Biophys. Acta. 1969; 190:264–273. [PubMed: 4900574]

Sato T, Katagiri K, Yokonishi T, Kubota Y, Inoue K, Ogonuki N, Matoba S, Ogura A, Ogawa T. *In vitro* production of fertile sperm from murine spermatogonial stem cell lines. Nat. Commun. 2011; 2:472. [PubMed: 21915114]

Schibler U, Kelley DE, Perry RP. Comparison of methylated sequences in messenger RNA and heterogeneous nuclear RNA from mouse L cells. J. Mol. Biol. 1977; 115:695–714. [PubMed: 592376]

Scott LJ, Mohlke KL, Bonnycastle LL, Willer CJ, Li Y, Duren WL, Erdos MR, Stringham HM, Chines PS, Jackson AU, et al. A genome-wide association study of type 2 diabetes in Finns detects multiple susceptibility variants. Science. 2007; 316:1341–1345. [PubMed: 17463248]

Sedgwick B. Repairing DNA-methylation damage. Nat. Rev. Mol. Cell Biol. 2004; 5:148–157. [PubMed: 15040447]

Shah JC, Clancy MJ. *IME4*, a gene that mediates *MAT* and nutritional control of meiosis in *Saccharomyces cerevisiae*. Mol. Cell. Biol. 1992; 12:1078–1086. [PubMed: 1545790]

Shaha C, Tripathi R, Mishra DP. Male germ cell apoptosis: regulation and biology. Philos. Trans. R. Soc. Lond. B Biol. Sci. 2010; 365:1501–1515. [PubMed: 20403866]

Shalini S, Bansal MP. Role of selenium in spermatogenesis: differential expression of cjun and cfos in tubular cells of mice testis. Mol. Cell. Biochem. 2006; 292:27–38. [PubMed: 17066317]

Sharif J, Muto M, Takebayashi S, Suetake I, Iwamatsu A, Endo TA, Shinga J, Mizutani-Koseki Y, Toyoda T, Okamura K, et al. The SRA protein Np95 mediates epigenetic inheritance by recruiting Dnmt1 to methylated DNA. Nature. 2007; 450:908–912. [PubMed: 17994007]

Shi Y, Lan F, Matson C, Mulligan P, Whetstine JR, Cole PA, Casero RA, Shi Y. Histone demethylation mediated by the nuclear amine oxidase homolog LSD1. Cell. 2004; 119:941–953. [PubMed: 15620353]

Tahiliani M, Koh KP, Shen YH, Pastor WA, Bandukwala H, Brudno Y, Agarwal S, Iyer LM, Liu DR, Aravind L, Rao A. Conversion of 5-methylcytosine to 5-hydroxymethylcytosine in mammalian DNA by MLL partner TET1. Science. 2009; 324:930–935. [PubMed: 19372391]

Thalhammer A, Bencokova Z, Poole R, Loenarz C, Adam J, O'Flaherty L, Schödel J, Mole D, Giaslakiotis K, Schofield CJ, et al. Human AlkB homologue 5 is a nuclear 2-oxoglutarate dependent oxygenase and a direct target of hypoxia-inducible factor 1α (HIF-1α). PLoS ONE. 2011; 6:e16210. [PubMed: 21264265]

Trapnell C, Pachter L, Salzberg SL. TopHat: discovering splice junctions with RNA-Seq. Bioinformatics. 2009; 25:1105–1111. [PubMed: 19289445]

Trapnell C, Williams BA, Pertea G, Mortazavi A, Kwan G, van Baren MJ, Salzberg SL, Wold BJ, Pachter L. Transcript assembly and quantification by RNA-Seq reveals unannotated transcripts and isoform switching during cell differentiation. Nat. Biotechnol. 2010; 28:511–515. [PubMed: 20436464]

Trewick SC, Henshaw TF, Hausinger RP, Lindahl T, Sedgwick B. Oxidative demethylation by *Escherichia coli* AlkB directly reverts DNA base damage. Nature. 2002; 419:174–178. [PubMed: 12226667]

Tsukada Y, Fang J, Erdjument-Bromage H, Warren ME, Borchers CH, Tempst P, Zhang Y. Histone demethylation by a family of JmjC domain-containing proteins. Nature. 2006; 439:811–816. [PubMed: 16362057]

van den Born E, Vågbø CB, Songe-Møller L, Leihne V, Lien GF, Leszczynska G, Malkiewicz A, Krokan HE, Kirpekar F, Klungland A, Falnes PØ. ALKBH8-mediated formation of a novel diastereomeric pair of wobble nucleosides in mammalian tRNA. Nat. Commun. 2011; 2:172. [PubMed: 21285950]

Wei CM, Gershowitz A, Moss B. 5′-Terminal and internal methylated nucleotide sequences in HeLa cell mRNA. Biochemistry. 1976; 15:397–401. [PubMed: 174715]

Yi CQ, Jia GF, Hou GH, Dai Q, Zhang W, Zheng GQ, Jian X, Yang CG, Cui QA, He C. Iron-catalysed oxidation intermediates captured in a DNA repair dioxygenase. Nature. 2010; 468:330–333. [PubMed: 21068844]

Zhong S, Li H, Bodi Z, Button J, Vespa L, Herzog M, Fray RG. MTA is an *Arabidopsis* messenger RNA adenosine methylase and interacts with a homolog of a sex-specific splicing factor. Plant Cell. 2008; 20:1278–1288. [PubMed: 18505803]

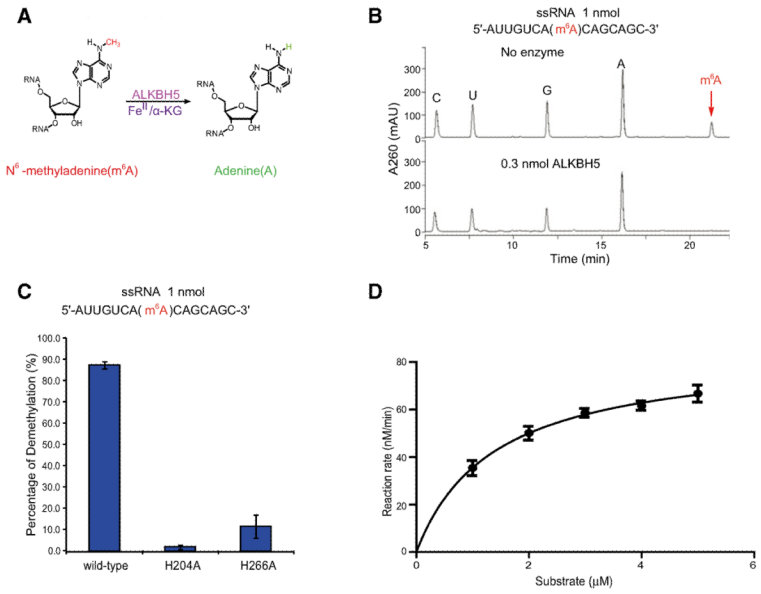

Figure 1. ALKBH5 Catalyzes Demethylation of m^{6}A-Containing ssRNA

(A) Proposed oxidative demethylation of m^{6}A to adenosine in RNA by ALKBH5.

(B) ALKBH5 (0.3 nmol) completely demethylated m^{6}A in ssRNA (1 nmol) at pH 7.5 and 16°C overnight as revealed by HPLC analysis of the digested substrates.

(C) Demethylation activity of m^{6}A-containing ssRNA for the wild-type ALKBH5 (WTALKBH5) and ALKBH5 mutants, H204A and H266A, at pH 7.5 and 16°C for 12 hr. Error bars indicate ± SEM (n = 3).

(D) Michaelis-Menten plot of the steady-state kinetics of ALKBH5-catalyzed demethylation of m^{6}A in ssRNA at pH 7.5 at room temperature. Error bars indicate ± SEM (n = 3). See also Figure S1 and Table S1.

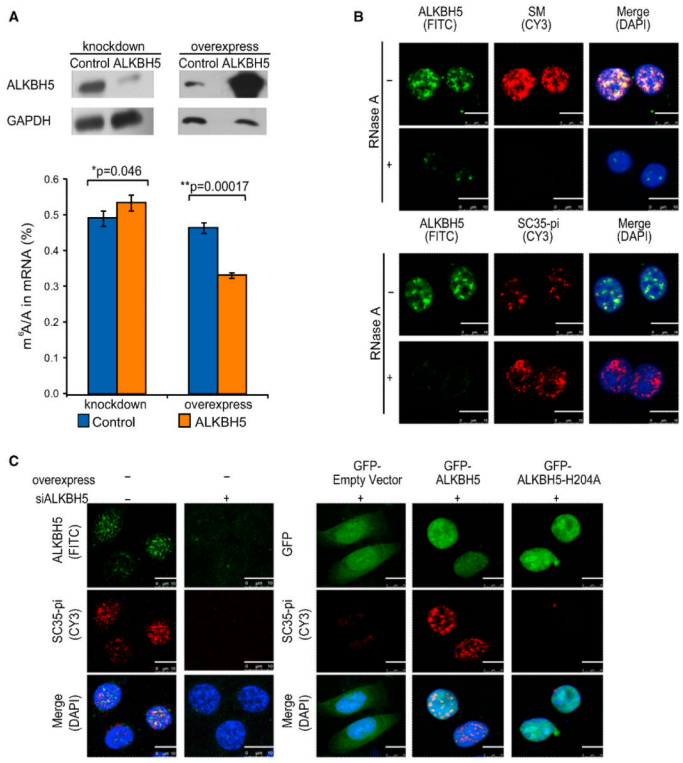

Figure 2. Demethylation of m^{6}A in mRNA by ALKBH5 and Its Effects on Selected mRNA Splicing Factors in HeLa Cells

(A) Top panel, western blotting of ALKBH5 upon knockdown and overexpression of ALKBH5 in HeLa cells. GAPDH served as a loading control. Bottom panel, quantification of the m^{6}A/A ratio in mRNA using LC-MS/MS. Both sets of data were assessed using Student's t test. Error bars indicate ± SEM (n = 8).

(B) RNase A-sensitive subcellular localization of ALKBH5 (green) in nuclear speckles. RNA processing factors SM and SC35-pi (red) were used as a nuclear speckle marker. DAPI (blue): DNA staining. Scale bar: 10 μm.

(C) ALKBH5-dependent nuclear speckle staining of SC35-pi. ALKBH5 deficiency led to diminished signal of SC35-pi (red), which could be restored by over-expression of GFP-tagged WT ALKBH5, but not by the empty vector or the inactive mutant H204A. DAPI (blue): DNA staining. Scale bar: 10 μm. Representative images from one of the three independent experiments were shown for (B) and (C). See also Figure S2.

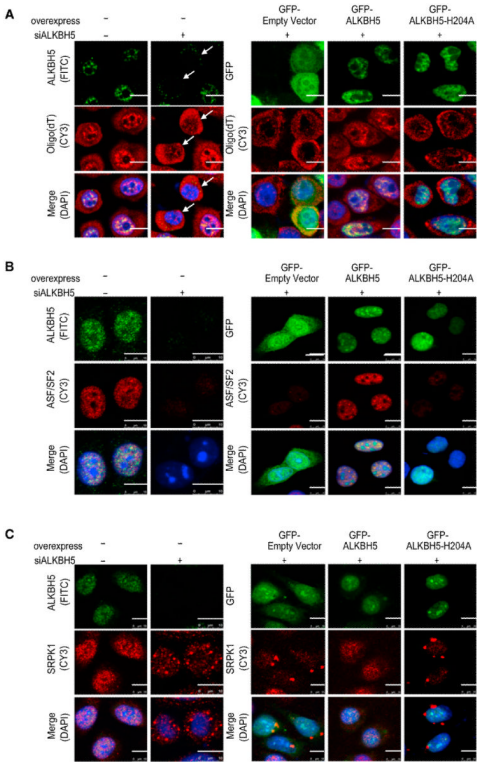

Figure 3. ALKBH5-Mediated Demethylation Affects mRNA Export

(A) Poly(A)-RNA-FISH using oligo(dT)$_{50}$-digoxigenin probe was performed in control and ALKBH5-deficient cells. mRNA (red) was mainly detected in the nucleus of control cells while in the cytoplasm of ALKBH5-deficient cells. Overexpression of GFP-tagged WT ALKBH5, but neither the empty vector nor the inactive ALKBH5 H204A, could rescue the nuclear mRNA export induced by endogenous ALKBH5 depletion. Arrows indicate ALKBH5-deficient cells.

(B) ALKBH5-dependent nuclear speckle staining of ASF/SF2. ALKBH5 deficiency led to diminished signal of the ASF/SF2 (red), which could be efficiently restored by overexpression of GFP-tagged WT ALKBH5, but not by the empty vector or H204A mutant.

(C) Aberrant localization of SRPK1 in ALKBH5-depleted HeLa cells. SRPK1 (red) was mainly detected in the nucleus of control cells. It was relocalized to form dot-like signals in the cytoplasm after ALKBH5 knockdown. The native localization could be rescued by overexpression of GFP-tagged WT ALKBH5, but not by the empty vector or inactive H204A mutant. DAPI (blue): DNA staining. Scale bar: 10 mm. Representative images from one of three independent experiments were shown. See also Figure S3.

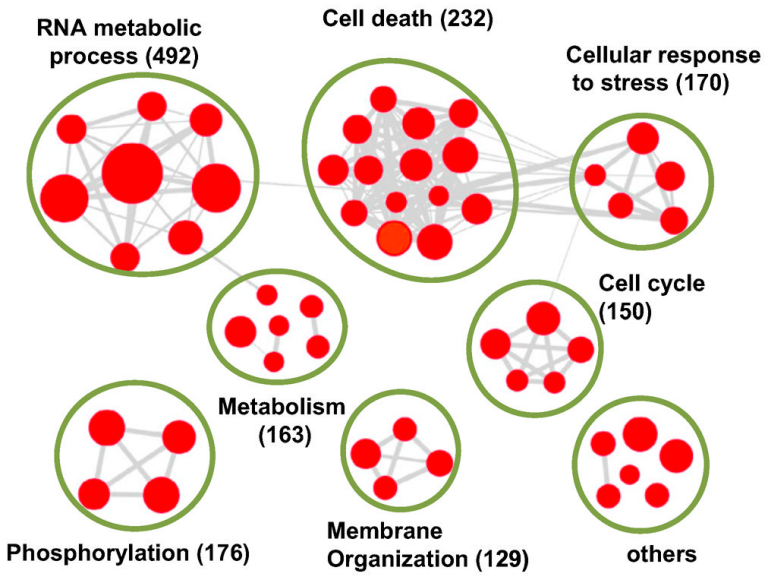

Figure 4. Gene Ontology and Enrichment Analysis of DEGs from HeLa RNA-Seq

A total of 2,740 DEGs at either gene or isoform levels were subjected to DAVID GO analysis. An enrichment map was constructed by using Cytoscape installed with the Enrichment Map plugin. Red node represents each enriched GO pathway ($p < 0.01$, FDR $q < 0.05$, overlap cutoff > 0.5). Node size is proportional to the total number of genes in each pathway. Edge thickness represents the number of overlapping genes between nodes. GO pathways of similar functions are sorted into one cluster, marked with circles and labels. Gene numbers in each cluster are labeled. See also Figure S4 and Tables S2, S3, and S4.

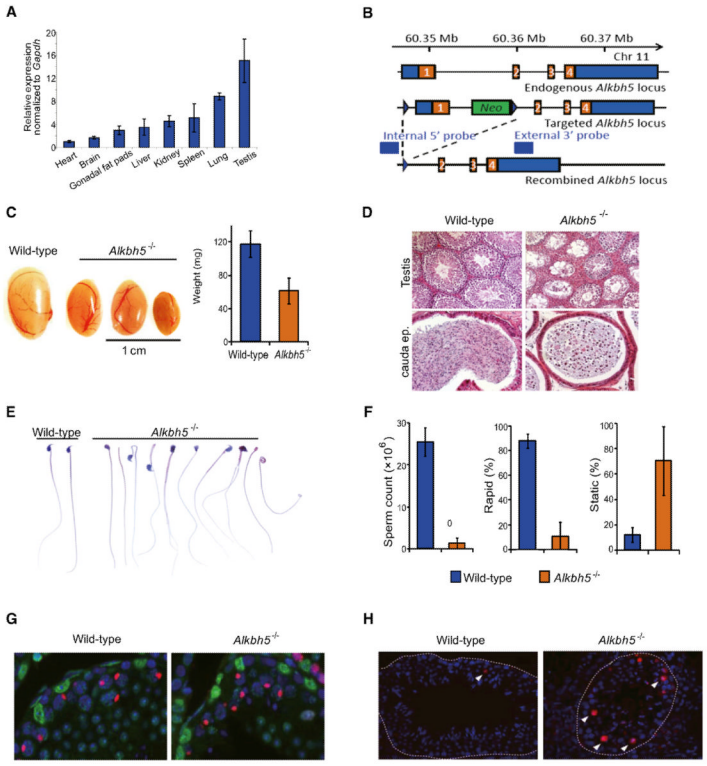

Figure 5. Spermatogenic Defects in *Alkbh5*-Deficient Mice

(A) Relative expression of *Alkbh5* in different organs. The testis is the organ with the highest expression of *Alkbh5* mRNA. Data are presented as an expression relative to the expression in heart, set to one, and normalized to *Gapdh* expression in each organ. Error bars indicate ± SEM (n = 3 individual mice, each with duplicate cDNA synthesis and triplicate RT-qPCR).

(B) Overview of the *Alkbh5*-targeting strategy.

(C) Left panel, representative testes from 12-week-old WT and *Alkbh5*$^{-/-}$ males. Right panel, average testis weight (mg) from 12-week-old WT (117.4 ± 16.0 mg, n = 12) and *Alkbh5*$^{-/-}$ (61.4 ± 15.5 mg, n = 20) males. Error bars indicate ± SEM.

(D) Hematoxylin and eosin stained sections from WT and *Alkbh5*$^{-/-}$ formalin-fixed and paraffin-embedded testes and cauda epididymis. Note the striking presence of round cells in the *Alkbh5*$^{-/-}$ cauda epididymis.

(E) Representative images of WT and *Alkbh5*$^{-/-}$ spermatozoa after staining with hematoxylin and eosin.

(F) Characterization of spermatozoa number and motility for WT and *Alkbh5*$^{-/-}$. Error bars indicate ± SEM (n = 4, wild-type, and n = 4, Alkbh5$^{-/-}$, individual mice).

(G) Immunofluorescence staining reveals an increased primary:secondary spermatocyte ratio in *Alkbh5*$^{-/-}$ as compared to WT testicular tubuli. Sertoli cell nuclei were stained bright green for H3K27me3. Pachytene-stage primary spermatocytes were stained with phosphorylated H2AX in red, where the foci represent sex bodies specific to the pachytene stage. Round spermatides (secondary spermatocytes) are seen as smaller round nuclei positioned further toward the lumen of seminiferous tubuli. The DNA was stained blue with DAPI.

(H) Increased cell death through apoptosis in *Alkbh5*-deficient testes compared to WT was apparent from TUNEL staining of formalin-fixed and paraffin-embedded testicular sections. See also Figure S5.

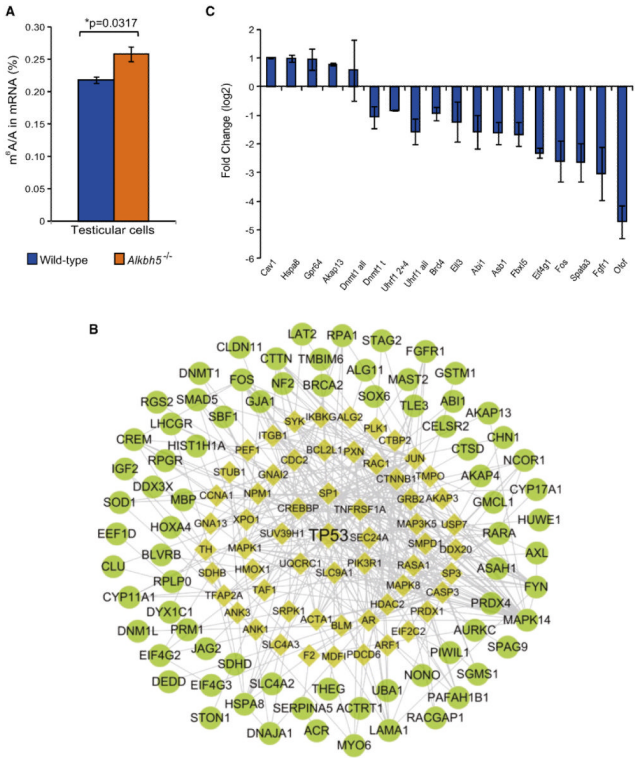

Figure 6. Transcriptome Analysis of Mouse Testicular Cells

(A) Quantification of the m^6A/A ratio in mouse testicular cells by LC-MS/MS. Data were assessed using Welch t test to account for difference between variances due to the increased variation between *Alkbh5*$^{-/-}$ mice in the representation of spermatogenic cell. Error bars indicate ± SEM (n = 2 WT and n = 5 *Alkbh5*$^{-/-}$ mice).

(B) A simplified scheme showing the functional interaction network between p53 and Alkbh5 transcriptome involved in apoptosis. A total of 127 spermatogenesis-related, differentially expressed genes were applied to Cytoscape analysis (version 2.8.2) installed with Reactome FI plugin. A total of 78 genes fall into p53 functional interaction network via the connection of 60 linker genes. Circle, differentially expressed genes from RNA-seq of Alkbh5; diamond, linker.

(C) RT-qPCR validation of spermatogenesis- and apoptosis-related genes and isoforms found to be differentially expressed in *Alkbh5*-deficient testicular cells compared to those in the WT testicular cells. Expression of all genes was normalized to *Actb*, and WT expression was set to 1. Error bars indicate ± SEM (n = 3–5 individual mice, each with triplicate RT-qPCR). See also Figure S6 and Tables S5 and S6.